Structure of mirror pairs ^{8}Li-^{8}B and ^{9}Be-^{9}B in Fermionic Molecular Dynamics

IOP Conf. Series: Journal of Physics: Conf. Series **1023** (2018) 012012 doi:10.1088/1742-6596/1023/1/012012

Structure of mirror pairs ^{8}Li-^{8}B and ^{9}Be-^{9}B in Fermionic Molecular Dynamics

K. R. Henninger

iThemba Laboratory for Accelerator Based Sciences, Old Faure road, Western Cape, South Africa

E-mail: katharinehenninger@gmail.com

Abstract. Structure of light weakly-bound nuclei like ^{8}B or ^{9}Be is of astrophysical interest. Microscopic models of their structure face challenges, since these nuclei feature clusters; difficult to access using a basis of spatially-isotropic single-particle states. The Fermionic Molecular Dynamics (FMD) model offers a basis general enough to describe both compact (shell model like) states and clustering. We discuss FMD calculations for the mirror pairs ^{8}B-^{8}Li and ^{9}Be-^{9}B. These are interesting because one nucleus of each pair is weakly-bound or unbound. It is shown that the FMD calculations reproduce energy levels and radii fairly, and that subtraction of the Coulomb energy calculated from the FMD states restores degeneracy of the mirror levels within at most $\sim$ 100 keV.

1. Introduction

Weakly-bound nuclei have low-lying states proximal to thresholds for decay by particle emission. This means that, according to the Ikeda hypothesis [1], the asymptotic part of the wave function for these states will be well-described by clustering configurations.

Mirror nuclei are systems of nucleons that would be degenerate in energy were it not for isospin-symmetry breaking in the NN interaction: effectively, without the Coulomb interaction (the primary breaker of isospin symmetry). The Coulomb interaction and the uniformity of the charge distribution in the nucleus are connected [2]. Thus, structural differences between mirror nuclei (such as different clustering) can be considered as mainly driven by the Coulomb interaction, and show up in the location of decay thresholds relative to different states. For example, in ^{8}B, the ^{7}Be+p threshold is $\approx$ 0.3 MeV above the ground state, but the corresponding ^{7}Li+n threshold is $\approx$ 3 MeV above the ^{8}Li ground state. By the Ikeda hypothesis, this suggests different asymptotic structure of these levels, *i.e.* different clustering. If we can account for these structural differences when calculating Coulomb energy, does subtracting it restore degeneracy of mirror energy levels? In this paper, we try to answer this question for the mirror nuclei ^{8}Li-^{8}B and ^{9}Be-^{9}B; pairs which are of interest to astrophysics (*e.g.* [3, 4]).

Clusters are difficult to model when beginning from spatially-isotropic single-particle distributions [5]. In this study we use the Fermionic Molecular Dynamics (FMD) model [6]. FMD offers a Hilbert space in which clustering may either be introduced explicitly, or arise naturally in the basis states, allowing one to access both compact and clustering configurations

consistently [5]. Another highlight of FMD is its treatment of the proton-neutron mass difference: while many models neglect this, it is taken into account in FMD [5], making comparison of energy-levels in mirror nuclei possible. The model is outlined in Section 2.

2. Fermionic Molecular Dynamics

Starting with protons and neutrons as basic constituents of a nuclear system, we choose intrinsic many-body configurations $|Q\rangle$ that are Slater determinants of single-particle states $|q\rangle$, or [7]:

$$|Q\rangle = \hat{\mathcal{A}}\left\{|q_1\rangle \otimes ... \otimes |q_A\rangle\right\} \tag{1}$$

where $\hat{\mathcal{A}}$ is the antisymmetrization operator and $Q = \{q_1, ..., q_A\}$ denotes the set of single-particle parameters. The single-particle states corresponding to the protons and neutrons are:

$$|q\rangle = \sum_i |a_i, \vec{b}_i\rangle \otimes |\chi_i^{\uparrow}, \chi_i^{\downarrow}\rangle \otimes |\xi\rangle c_i, \tag{2}$$

Parameters $\vec{b}$ relate to the mean position and mean momentum and and a to the width of the wave-packets [8] respectively. The ket $|\chi^{\uparrow}, \chi^{\downarrow}\rangle$ allows all possible orientations of the nucleon spin. The isospin is defined in $|\xi\rangle$. In co-ordinate space one has Gaussian wave-packets:

$$\langle\vec{x}|a, \vec{b}\rangle = \exp\left\{-\frac{(\vec{x}-\vec{b})^2}{2a}\right\}. \tag{3}$$

Slater determinants $|Q\rangle$ like that in Eq.(1) are in general not eigenstates of the angular momentum or parity operators, so these need to be projected out via projection operators [8]:

$$\hat{P}^{\pi} = \frac{1}{2}(1 + \pi\hat{\Pi}) \tag{4a}$$

$$\hat{P}^{J}_{MK} = \frac{2J+1}{8\pi^2}\int d\Omega\, D^{J}_{MK}(\Omega)^{*}\hat{R}(\Omega), \tag{4b}$$

where $D^{J}_{MK}(\alpha, \beta, \gamma)$ is the Wigner D-matrix, $\hat{R}(\alpha, \beta, \gamma) = e^{-i\alpha\hat{J}_z}e^{-i\beta\hat{J}_y}e^{-i\gamma\hat{J}_z}$ is the rotation operator and $\hat{\Pi}$ is the parity operator. The $\Omega = \{\alpha, \beta, \gamma\}$ symbolizes the three Euler angles. The projected states are such that the result is a many-body state with quantum numbers J, K, M. By diagonalizing the Hamiltonian in the set of K-projected states,we obtain the FMD many-body basis states

$$|Q; J^{\pi}M\alpha\rangle = \sum_K |Q; J^{\pi}MK\rangle c_K^{J^{\pi}\alpha}. \tag{5}$$

Additional basis states can be generated by performing minimization subject to constraints. These constraints could be on *e.g.* radii, moments or deformation parameters [5]. One may also create explicit cluster states: States which are antisymmetrized product states of Slater determinants derived via the above-described minimization scheme, *i.e.*

$$|Q_{c1+c2}\rangle = \hat{\mathcal{A}}\left\{|Q_{c1}\rangle \otimes |Q_{c2}\rangle\right\}. \tag{6}$$

The Hamiltonian is then diagonalized in this basis set, and one obtains the eigenstates. As already mentioned, the FMD takes account of the proton-neutron mass difference, setting the mass of a proton to 938.27231 MeV and the mass of a neutron to 939.56563 MeV.

2.1. Coulomb energy
In the FMD, matrix elements for a two-body $\frac{1}{r}$ interaction like the Coulomb interaction are [5]:

$$\langle a_\kappa \vec{b}_\kappa, a_\lambda \vec{b}_\lambda | \frac{1}{r} | a_\mu \vec{b}_\mu, \alpha_\nu \vec{b}_\nu \rangle = R_{\kappa\mu} R_{\lambda\nu} \frac{1}{\sqrt{\rho^2_{\kappa\lambda\mu\nu}}} \mathrm{erf} \left\{ \sqrt{\frac{\rho^2_{\kappa\lambda\mu\nu}}{2\alpha_{\kappa\lambda\mu\nu}}} \right\}. \quad (7)$$

where all the terms are as defined in [5], and "erf" is the Error Function.

This determination of Coulomb energy allows it to be extracted from the structural information in our calculations and does not rely on (extreme) approximations to the nucleon distribution, as does the well-known uniform sphere approximation used in the Semi-Empirical Mass Formula (SEMF, or Bethe-Weizsäcker formula):

$$E_{SEMF} = a_C \frac{Z(Z-1)}{A^{1/3}}, \quad (8)$$

where a_C is 0.691 MeV [9]. Comparing this value to one obtained in Eq.(7) can be interesting, as how much the two deviate is a good indicator of how "non uniform" or "non-spherical" a charge distribution is.

3. Calculations
The basis sets used for these calculations comprised FMD VAP states with constraints on the matter radius, projected on the angular momenta and parties of the ground state and first two excited states of the nuclei of interest. The states to be included in each basis were then chosen by an optimization process [10]. To these states were added explicit cluster configurations corresponding to the lowest-lying thresholds (listed in Table 1). In each cluster configuration, the core consisted of a single VAP state projected onto the angular momentum and parity of the core's ground state.

To create equivalent model spaces for the mirror nuclei, it was decided to use the basis states of the mirror, with protons and neutrons exchanged. This gives a total basis size of up ≈40 VAP states and 11 explicit cluster configurations in each basis set.

Table 1. Summary of the cluster configurations included in the basis sets for each nucleus.

Nucleus	Clustering
^{8}Li	^{7}Li+n
^{8}B	^{7}Be+p
^{9}Be	^{8}Be+n
^{9}B	^{8}Be+p

The Argonne *v18* interaction [11] was used, transformed by the Unitary Correlation Operator Method (UCOM) [12]. The transformation enables the inclusion of short-range central and tensor correlations. Three-body and higher-order terms are not included.

4. Results
Calculated level-schemes are provided in Fig. 1, where they are compared to the experimental levels-schemes. In all cases, one sees under-binding in our calculations, which is primarily a

feature of the interaction used [13]. The important calculated quantity is thus binding relative to the calculated thresholds, which compares fairly with experiment. Thresholds were calculated within an FMD model space of comparative size to that of the calculations, and also using the same interaction.

In Fig. 1, one may also note that the higher-lying levels in all four systems are somewhat more poorly-reproduced than the lower-lying levels (*e.g.* note the 0^+ states of ^{8}Li and ^{8}B). This is because the bases described above (Section 3) are not adequately large to accurately reproduce the high-lying states ($\approx$ 10 MeV) in any of these nuclei, as these states may be broad resonances or strongly mixed with the continuum [14], and are thus unlikely to be well-described in a model space that can accurately describe the lower-lying states.

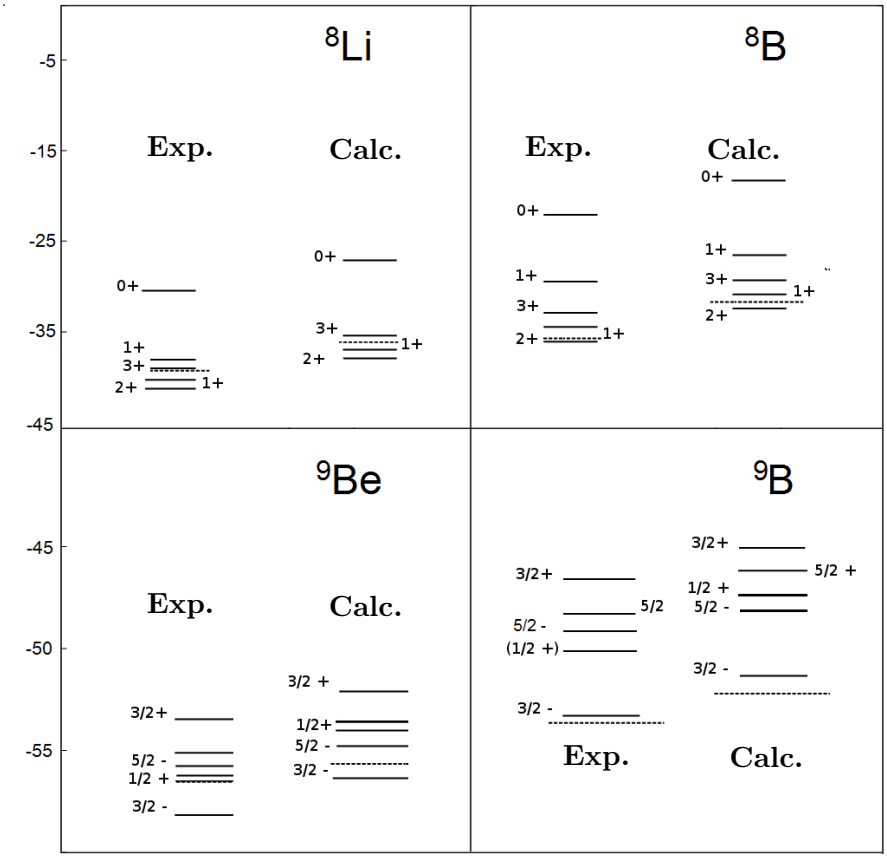

Figure 1. Experimental and calculated energy levels (labeled Exp. and Calc. respectively). Dotted lines indicate the lowest-lying thresholds. Note reproduction of binding energy relative to threshold. Calculations are labeled for the respective nuclei. For A=9 mirror nuclei (bottom panels), note that the $5/2^-$ and $1/2^+$ levels are reversed in order in our calculations. The $1/2^+$ state is very broad ($\approx$ 0.3 MeV broad in ^{9}Be, and $\approx$ 3 MeV broad in ^{9}B [14]), explaining the better reproduction of the $5/2^-$ state in this model-space.

Good indicators of whether structure is being effectively reproduced by the calculations are the calculated matter- and charge-radii. Table 2 compares the matter- and charge-radii (where known) with experiment. Note the difference between the calculated matter- and charge radii

IOP Conf. Series: Journal of Physics: Conf. Series **1023** (2018) 012012 doi:10.1088/1742-6596/1023/1/012012

of ^{8}B, indicative of the fact that we reproduce a proton halo in our calculations. This indicates that the calculations capture the structural features of ^{8}B, at least in the ground state.

Table 2. Calculated matter- and charge-radii, compared to experiment. Note the difference between the matter- and charge radii of ^{8}B, indicative of a proton halo.

Nucleus	Matter radius [fm]		Charge radius [fm]	
	Exp. [a]	Calc. C	Exp.[b]	Calc. C
^{8}Li	2.37(2)	2.243	2.29(8)	2.211
^{8}B	2.38(4)	2.282	-	2.537
^{9}Be	2.38(1)	2.338	2.519(12)	2.417
^{9}B	-	2.358	-	2.556

[a]All experimental matter radii from [14].

[b]Charge radius of ^{8}Li from [15], and for ^{9}Be from [16].

In Figs. 2, the effect of subtraction of the Coulomb energies is demonstrated graphically. As described in the caption, plots illustrate the effect of subtracting the Coulomb energy calculated firstly using the Semi-Empirical Mass Formula, and then that calculated from the FMD states as described in Sect. 2.1. It can clearly be seen that subtraction of the "FMD Coulomb energy" comes close to restoring the degeneracy of the analogous energy levels, both in the case of the $A = 8$ and $A = 9$ systems.

To be more precise, the difference between calculated energies of the analog states in the $A = 8$ system is of the order of 100 keV (see Table 3), while for the $A = 9$ system, it is of the order of tens of keV. A tentative explanation of why the method seems more effective for the $A = 9$ systems is that both ^{9}Be and ^{9}B are probably modeled equally well (or badly!) in model-spaces of the size used (both have quite complicated three-body structure even in the ground state [14], meaning that they are both hard to access in a limited model space), while for the $A = 8$ group, it may be argued that our approximation is worse for ^{8}B than for ^{8}Li (since ^{8}Li has a "simpler" structure (see *e.g.* [14]), leading to a greater discrepancy in the results due to a failure to capture some structural information in ^{8}B.

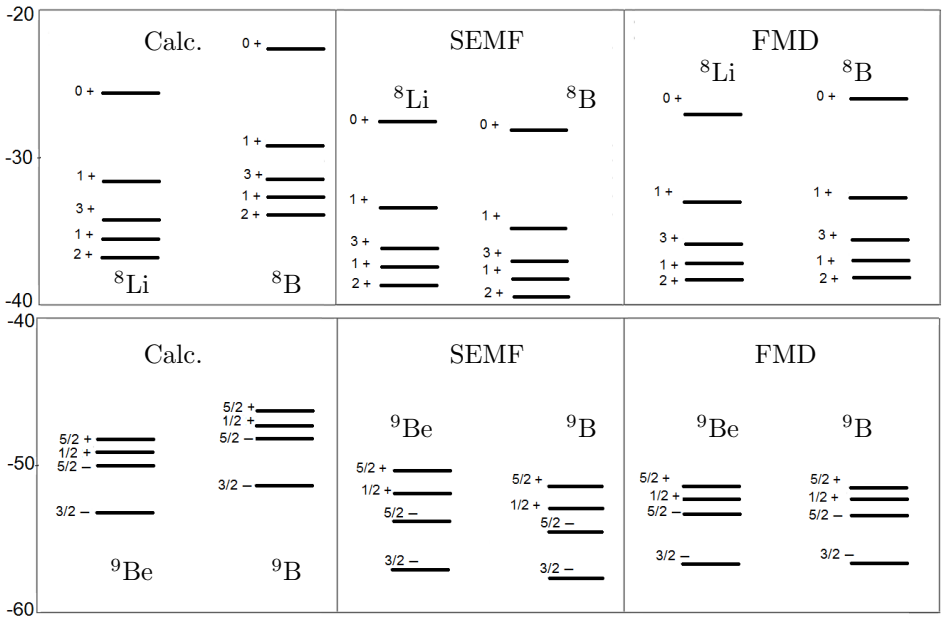

Figure 2. Calculated energy levels for the A=8 and $A = 9$ mirror systems (labeled Calc.), shown before and after subtraction of the SEMF Coulomb energy and the FMD Coulomb energy (in panels labeled SEMF and FMD, respectively). Levels are labeled for the nuclei for which they are calculated. Note how close to degenerate the levels become after subtraction of the FMD Coulomb energy.

Level	Energy less FMD Coulomb [MeV]	Energy less SEMF Coulomb [MeV]	Diff. FMD (Abs.) [MeV]	Diff. SEMF (Abs.) [MeV]
^{8}Li 2+	-38.050	-38.376		
^{8}B 2+	-37.907	-39.700	0.143	1.324
^{8}Li 1+	-36.412	-36.754		
^{8}B 1+	-36.249	-38.130	0.163	1.376
^{9}Be 3/2 -	-56.661	-57.351		
^{9}B 3/2 -	-56.603	-58.147	0.058	0.796
^{9}Be 1/2 +	-52.265	-53.195		
^{9}B 1/2 +	-52.219	-54.209	0.046	1.014
^{9}Be 5/2 -	-53.382	-54.120		
^{9}B 5/2 -	-53.322	-54.949	0.060	0.829
^{9}Be 5/2 +	-51.403	-52.355		
^{9}B 5/2 +	-51.351	-53.331	0.052	0.976

Table 3. The differences in calculated energy of analogous energy levels before and after subtraction of the FMD Coulomb energy (column 2) and the SEMF Coulomb energy (column 3). Note that the degeneracy is restored by $\sim$ 10 keV for the $A = 9$ systems and by $\sim$ 100 keV for the $A = 8$ systems.

5. Summary and Conclusion

The FMD calculations of energy and matter- and charge-radii for the ^{8}Li-^{8}B and ^{9}Be-^{9}B systems compare, for the most part, favorably with experiment. The subtraction of a Coulomb energy "based on structure", or one which takes into account the asymptotic structure of these nuclei, has been shown to restore degeneracy of the mirror levels with at most ~ 100 keV.

As the FMD does take into account the proton-neutron mass difference, the results presented here indicate that the major differences between the energies of the mirror nuclei are brought about by structural considerations arising through the Coulomb interaction. This conclusion is probably unsurprising, but is interesting for drip-line physics where it is important to know to what extent the proton:neutron ratio plays a role, through what mechanism it plays a role, and how to account for it.

As an extension to this study, it must also be noted that the UCOM-transformed AV18 interaction used is truncated at two-body level. The missing three-body strength is accounted for by using a coefficient of 2 for the spin-orbit force. Investigations of the effect of three-body terms would be worth carrying out.

6. References

[1] Ikeda K, Takigawa N and Horuichi H 1968 Prog. Theor. Phys. *(Japan)* **Supplement** 464
[2] Sagawa H 2007 J. Phys. **G349** 949
[3] Reeves H and Meyer J P 1978 Astrophys. J **226** 613
[4] Parker P D 1966 Phys. Rev. **150** 851
[5] Neff T and Feldmeier H 2010 *Cluster Structure in the Fermionic Molecular Dynamics Approach Cluster Structure of Atomic Nuclei* ed Brenner M (Research Signpost publishing) pp 67–94
[6] Feldmeier H 1990 Nucl. Phys. **A515** 147
[7] Feldmeier H and Schnack J 1997 Prog. Part. Nucl. Phys. **39** 343
[8] Neff T and Feldmeier H 2008 Eur. Phys. J. **156** 69
[9] Wong S S M 2002 *Introductory Nuclear Physics* (New Jersey: Pearson Prentice-Hall publishers) pp 11-13, 261-274 and 372-375.
[10] Henninger K R 2016 J. Phys. Conf. Ser. **724** 012019
[11] Wiringa R B, Stokes B G J and Schiavilla R 1995 Phys. Rev ***C*** **51** 38
[12] Roth R, Hergert H, Papakonstantinou P, Neff T and Feldmeier H 2005 *Phys. Rev.* ***C*** **72** 034002
[13] Dickhoff W H 2016 IOP: Conf. Ser. **702** 012013
[14] Tilley D R, Kelley H, Godwin J L, Millener D J, Purcell J E, Sheu C G and Weller H R 2004 (revised 2014) Nucl. Phys. **A745** 155
[15] Ewald G, Nörtershäuser W, Dax A, Götte S, Kirchner R, Kluge H J, Kühl T, Sanchez R, Wojtaszek A, Bushaw B A, Drake G W F, Yan Z C and Zimmermann C 2004 Phys. Rev. Lett. **93** 113002
[16] Nörtershäuser W, Tiedemann D, Žáková M, Andjelkovic Z, Blaum K, Bissell M L, Cazan R, Drake G W F, Geppert C, Kowalska M, Krämer J, Krieger A, Neugart R, Sánchez R, Schmidt-Kaler F, Yan Z C, Yordanov D T and Zimmermann C 2009 *Phys. Rev. Lett.* **102**(6) 062503 URL `https://link.aps.org/doi/10.1103/PhysRevLett.102.062503`